Regulation of Cell Death and Innate Immunity by Two Receptor-like Kinases in *Arabidopsis*

Minghui Gao,[1,2] Xia Wang,[2] Dongmei Wang,[3,4] Fang Xu,[2] Xiaojun Ding,[2] Zhibin Zhang,[2] Dongling Bi,[2] Yu Ti Cheng,[3] She Chen,[2] Xin Li,[3] and Yuelin Zhang[2,*]
[1]College of Biological Sciences, China Agricultural University, Beijing 100094, China
[2]National Institute of Biological Sciences, Zhongguancun Life Science Park, Beijing 102206, China
[3]Michael Smith Laboratories, University of British Columbia, Vancouver V6T 1Z4, Canada
[4]Present address: Institute of Nuclear and Biotechnology, Xinjiang Academy of Agricultural Sciences, Urumuqi, China
*Correspondence: zhangyuelin@nibs.ac.cn
DOI 10.1016/j.chom.2009.05.019

SUMMARY

Upon recognition of bacterial flagellin, the plant receptor FLS2 heterodimerizes with brassinosteroid insensitive 1-associated receptor kinase 1 (BAK1) and activates plant defense responses. Because constitutive activation of defense responses is detrimental, plant resistance signaling pathways must be negatively controlled, although the mechanisms involved are unclear. We identified Arabidopsis BIR1 as a BAK1-interacting receptor-like kinase. Knocking out *BIR1* leads to extensive cell death, activation of constitutive defense responses, and impairment in the activation of MPK4, a negative regulator of plant resistance (R) protein signaling, by flagellin. *sobir1-1*, a mutant obtained in a screen for suppressors of the *bir1-1* phenotype, rescued cell death observed in *bir1-1*. *SOBIR1* encodes another receptor-like kinase whose overexpression activates cell death and defense responses. Our data suggest that *BIR1* negatively regulates multiple plant resistance signaling pathways, one of which is the *SOBIR1*-dependent pathway identified here.

INTRODUCTION

Plants rely solely on innate immunity to combat pathogen infections, as they do not have adaptive immune systems like animals (Jones and Dangl, 2006). There are two types of innate immune responses in plants. One is pathogen-associated molecular pattern (PAMP)-triggered immunity. PAMPs are conserved microbial components that elicit pathogen immune responses when recognized by the host receptors. The second type of innate immunity is effector-triggered immunity, which is evolved by plants to detect pathogen effectors and initiate defense responses to inhibit pathogen growth and restrict pathogen spread.

Two well-studied plant receptors of PAMPs, FLS2 and EFR, are members of the receptor-like kinase (RLK) family (Gomez-Gomez and Boller, 2000; Zipfel et al., 2006). RLK family is the largest group of protein kinases in plants. A typical RLK contains an extracellular ligand-binding sequence, a transmembrane region, and a C-terminal intracellular protein kinase domain. FLS2 recognizes the peptide flg22 from bacterial flagellin, while EFR recognizes a peptide derived from bacterial translation elongation factor EF-Tu. Recently, FLS2 was found to heterodimerize with brassinosteroid insensitive 1 (BRI1)-associated receptor kinase 1 (BAK1) in the perception of flagellin (Chinchilla et al., 2007; Heese et al., 2007). *bak1* mutant plants exhibited reduced sensitivity to flagellin in growth assays and are impaired in responsiveness to flagellin. BAK1 was originally identified as a BRI1 interactor, and it forms a protein complex with BRI1 during perception of Brassinosteroids (BRs) (Li et al., 2002; Nam and Li, 2002). In addition, BAK1 was also found to negatively regulate a BR-independent cell-death pathway. *bak1* mutant plants develop spreading necrosis upon pathogen infections (Kemmerling et al., 2007). Double knockout mutant plants of *bak1* and *bak1-like 1* (*bkk1*) exhibit a seedling lethality phenotype and constitutive defense responses (He et al., 2007). BAK1 was also shown to be a target of bacterial effectors AvrPto and AvrPtoB (Shan et al., 2008).

Effector-triggered immunity is mediated by the host resistance (R) proteins. Recognition of pathogen effectors by R proteins can be either direct or indirect. The guard hypothesis explains the indirect recognition (Van der Biezen and Jones, 1998), where R proteins bind to host components important for innate immunity. Modifications of these host components by pathogen effectors can be sensed by the R proteins, leading to activation of defense responses.

Most R proteins belong to the NB-LRR (nucleotide-binding site leucine-rich repeats) group, which shares structural similarity to the NOD proteins in animals (Jones and Dangl, 2006). Downstream of R proteins, NDR1 was shown to be required for the signaling of CC-NB-LRR type of R proteins containing a coiled-coil region at the N terminus (Century et al., 1995), while EDS1, PAD4, and SAG101 are required for the signaling by the TIR-NB-LRR type R proteins carrying an N-terminal Toll interleukin receptor domain (Aarts et al., 1998; Feys et al., 2005; Glazebrook et al., 1996; Parker et al., 1996).

R protein-mediated resistance is often accompanied by localized cell death, which may play important roles in the restriction of pathogen spread. Since constitutive activation of R proteins is detrimental to plant growth and development (Bendahmane et al., 2002; Mackey et al., 2003; Noutoshi et al., 2005; Shirano et al., 2002; Yang and Hua, 2004; Zhang et al., 2003a), R protein-mediated signaling pathways must be subject to tight

negative regulation to avoid activation of defense responses without pathogen attack.

Here, we report the identification of *bir1-1*, a mutant that constitutively activates defense responses similar to the autoactivated *R* gene mutants. *BIR1* encodes an RLK interacting with BAK1 in vivo. We carried out a suppressor screen of *bir1-1* and found that *sobir1-1* (*suppressor of bir1-1, 1*) strongly suppresses cell death in *bir1-1*. Combining the *sobir1* and *pad4-1* mutations leads to suppression of all mutant phenotypes of *bir1-1*, suggesting that *SOBIR1* functions in parallel with *PAD4*. *SOBIR1* encodes an RLK, probably functioning as a key regulator in a signal transduction pathway activated in *bir1-1* to promote cell death and disease resistance.

RESULTS

Identification of *bir1-1*

To identify important regulators of plant innate immunity, we carried out systematic reverse genetics analysis of genes whose transcript levels increased significantly 48 hr after inoculation with the bacterial pathogen *Pseudomonas syringae pv. maculicola* (*P.s.m.*) ES4326 (OD_{600} = 0.001). From initial analysis of homozygous knockout mutants of 200 genes (Table S1), one mutant was found to have a seedling lethality phenotype when grown at 22°C (Figure 1A), and none of the other T-DNA mutants has similar phenotypes. The mutant contains a T-DNA insertion in the third exon of *At5g48380*, which encodes an RLK (Figure 1B). We focused our analysis on this mutant because it has dramatic phenotypes, and *At5g48380* encodes an interesting protein most likely functioning in signal transduction. We later named it BAK1-interacting receptor-like kinase 1 (BIR1) due to its association with BAK1. BIR1 belongs to the LRRX group of RLKs (Figure S1) with 620 amino acids and 5 LRRs.

RT-PCR analysis of *BIR1* transcript in *bir1-1* mutant plants showed that the full-length cDNA of *BIR1* was no longer expressed (Figure S2A). Real-time RT-PCR analysis confirmed that *BIR1* is indeed induced by bacterial infection (Figure S2B). To determine whether the mutant phenotypes in *bir1-1* are caused by the T-DNA insertion, two additional T-DNA lines (SALK_008775 and WiscDsLox341G08) with insertions in the promoter region of *At5g48380* were analyzed. The expression of *At5g48380* is not affected by the T-DNA insertions, and no obvious mutant phenotype was observed in these two lines. So we transformed the wild-type *BIR1* gene into the *bir1-1* mutant to test whether it can complement the mutant phenotypes. As shown in Figure 1A, the wild-type *BIR1* reverted *bir1-1* completely back to wild-type, confirming that the seedling lethality phenotype was caused by the T-DNA insertion in *BIR1*. In addition, silencing *At5g48380* in wild-type background using artificial miRNA also caused a seedling lethality phenotype (data not shown).

Cell Death and Constitutive Defense Responses in *bir1-1*

Trypan blue staining was performed on mutant seedlings to test whether cell death occurred in *bir1-1*. Extensive cell death was found in both cotyledons and true leaves of the mutant plants, particularly along the veins (Figure S3A). We also performed 3, 3′-diaminobenzidine (DAB) staining on the *bir1-1* mutant seedlings. Strong staining was observed in *bir1-1* mutant plants
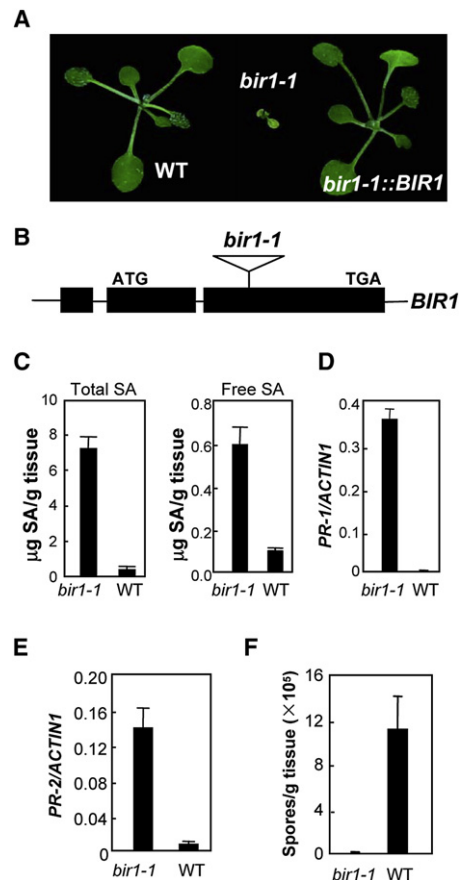

Figure 1. Characterization of the *bir1-1* Mutant

(A) Phenotypes of wild-type, *bir1-1*, and *bir1-1* transformed with a *BIR1* genomic clone. Plants were grown on soil at 22°C and photographed 3 weeks after planting.

(B) The T-DNA insertion site of *bir1-1* (WiscDsLox393-396D17) in *At5g48380*.

(C) SA accumulation in wild-type and *bir1-1* mutant seedlings. Levels of SA were determined as previously described (Li et al., 1999). Error bars represent SD from four measurements. Plants were grown on soil and sampled 3 weeks after planting.

(D and E) *PR-1* and *PR-2* expression in wild-type and *bir1-1* mutant seedlings. Total RNA was extracted from 2-week-old seedlings grown on 1/2 MS medium at 22°C. Relative levels of *PR-1* (D) or *PR-2* (E) were determined by real-time PCR using SYBR Green I chemistry as previously described (Zhang et al., 2003a). Values were normalized to the expression of *ACTIN1*. Error bars represent SD from three measurements.

(F) Growth of *H. parasitica* Noco2 on wild-type and *bir1-1* mutant plants. Two-week-old seedlings were sprayed with *H. parasitica* Noco2 spores (10^5 spores/ml). Infection was scored 7 days after inoculation by counting the number of conidiospores per gram of leaf samples. Error bars represent SD from the averages of three measurements.

(Figure S3B), indicating that the mutant seedlings accumulated high levels of H_2O_2 compared to the wild-type seedlings.

To test whether defense responses were constitutively activated in *bir1-1*, salicylic acid (SA) levels in *bir1-1* and wild-type plants were measured with high-performance liquid chromatography. *bir1-1* plants accumulated about 6-fold more free SA and about 20-fold more total SA (free SA plus glucose-conjugated SA) than wild-type controls (Figure 1C). In addition, high levels

of *PR-1* and *PR-2* were constitutively expressed in the mutant plants without induction (Figures 1D and 1E).

To test whether *bir1-1* mutant has enhanced pathogen resistance, *bir1-1* seedlings were challenged with the virulent oomycete pathogen *Hyaloperonospora parasitica* Noco2 (*H. p.* Noco2). As shown in Figure 1F, *bir1-1* seedlings displayed strong enhanced resistance against *H. p.* Noco2, suggesting that defense responses were constitutively activated in the *bir1-1* mutant plants.

Interestingly, the seedling lethality phenotype of *bir1-1* can be partially suppressed by growing the plants at high temperatures. *bir1-1* plants grown on soil at 28°C remain small, but can complete their life cycle and set seeds. When grown on Murashige and Skoog (MS) medium at 27°C, *bir1-1* plants were significantly bigger than those grown at 22°C (Figure S4A). Constitutive expression of *PR-1* and *PR-2* was also reduced at 27°C (Figures S4B and S4C).

To test whether all the *bir1-1* mutant phenotypes are caused by the T-DNA insertion in *BIR1*, *bir1-1* plants transformed with a genomic clone of *BIR1* were further analyzed in regards to its defense phenotypes. The wild-type *BIR1* complements the cell death phenotypes of *bir1-1* and suppressed the H_2O_2 accumulation in *bir1-1* (Figure S5A). The expression of *PR-1* and *PR-2* in the transgenic plants also reverted to wild-type levels (Figures S5B and S5C). In addition, the transgenic plants are no longer resistant to *H. p.* Noco2 (Figure S5D). Thus, all the mutant phenotypes observed in *bir1-1* can be complemented by *BIR1*.

BIR1 Is an Active Protein Kinase

To test whether BIR1 is an active protein kinase, the BIR1 cytoplasmic kinase domain was expressed in *E. coli* and tested for autophosphorylation activity. As shown in Figure S6A, the BIR1 kinase domain has autophosphorylation activity, indicating that BIR1 is an active protein kinase. To determine whether the kinase activity is important for its biological function, a mutant form of BIR1 kinase domain was created by mutating a conserved lysine (K331) to a glutamic acid (E331). This amino acid substitution was known to abolish kinase activity of other known RLKs (Horn and Walker, 1994; Li et al., 2002). The autophosphorylation activity of BIR1 kinase domain is dramatically reduced by the point mutation (Figure S6A). The K331E mutation was also introduced into a cDNA clone of *BIR1*. While wild-type *BIR1* cDNA can fully complement the *bir1-1* mutant phenotypes, the mutated gene can only partially complement the phenotypes of *bir1-1* (Figure S6B), suggesting that the kinase activity of BIR1 is important for its function.

## BIR1 Interacts with BAK1 on the Plasma Membrane

To determine the localization of the BIR1, *Arabidopsis* mesophyll protoplasts were transfected with a construct expressing the BIR1-GFP fusion protein under the cauliflower mosaic virus 35S promoter. As shown in Figure 2A, the BIR1-GFP fusion protein was localized to the plasma membrane, suggesting that BIR1 is a plasma membrane protein.

To identify proteins associated with BIR1, we generated transgenic plants expressing BIR1-3×FLAG fusion protein under its native promoter in the *bir1-1* mutant background. *bir1-1* plants expressing the BIR1-3×FLAG fusion protein displayed wild-type morphology (Figure S7A), suggesting that the fusion protein is

as functional as wild-type BIR1. A quantitative proteomics approach was previously used to identify specific components of protein complexes using isotope-coded affinity tag reagents and mass spectrometry (Ranish et al., 2003). To identify proteins specifically interacting with BIR1, we modified this method by labeling the protein in vivo using ^{15}N medium (Dong et al., 2007). The transgenic plants were plated on 1/2 MS plates with ^{15}N-labeled KNO_3 and NH_4NO_3 as sole nitrogen source while wild-type control plants were grown on regular 1/2 MS plates with ^{14}N KNO_3 and NH_4NO_3. After the seedlings were harvested, equal amounts of tissue from the transgenic plants and wild-type controls were mixed together for membrane isolation. Total protein from the membrane fraction was incubated with anti-FLAG agarose beads to selectively immunoprecipitate the FLAG-tagged BIR1. Proteins coimmunoprecipitated with BIR1-3×FLAG were subsequently analyzed by mass spectrometry. As shown in Figure S8, one of the peptides (LADGTLVAVK) identified is enriched in the ^{15}N fraction, suggesting that it is most likely from proteins specifically coimmunoprecipitated with BIR1-3×FLAG. Database search showed that this peptide is present in BAK1 and its close homologs SERK1 and SERK2. Probably due to low abundance of the BAK1 and SERK proteins, this peptide was the only one identified by mass spectrometry from these proteins. We did not find any other RLKs that specifically coimmunoprecipitate with BIR1-3×FLAG.

Next, we utilized a bimolecular fluorescence complementation (BiFC) approach (Walter et al., 2004) to test whether interactions between BAK1 and BIR1 can be visualized in vivo. In this experiment, BAK1 was fused to the N-terminal fragment of YFP (BAK1-YFP^N) while BIR1 was fused to the C-terminal fragment of YFP (BIR1-YFP^C). If BAK1 and BIR1 associate with each other, a fluorescent YFP complex would be formed. As shown in Figure 2B (top panel), YFP fluorescence was observed on the plasma membrane of *Arabidopsis* protoplasts cotransformed with the BAK1-YFP^N and BIR1-YFP^C constructs, suggesting that BAK1 and BIR1 interact with each other. We further tested the interactions between BIR1 and the BAK1 homologs, including BKK1, SERK1, and SERK2, using BiFC and found that BIR1 also interacts with these proteins on the plasma membrane. When the BIR1-YFP^C construct was cotransformed with BRI1-YFP^N, FLS2-YFP^N, or CLV1-YFP^N constructs, no YFP fluorescence was observed, suggesting that BIR1 does not interact with other RLKs like BRI1, FLS2, or CLV1. This is consistent with our observation that flg22-mediated growth inhibitions were not affected by the *bir1-1* mutation (Figure S9A). *bak1* and other BR mutants often have shorter hypocotyls when grown in the dark. Unlike the *bak1-4* seedlings, elongation of hypocotyls in *bir1-1 pad4-1* is similar to that in wild-type plants (Figure S9B).

Since cell death and defense responses were activated in both *bir1-1* and *bak1 bkk1* mutant plants and RLKs often function through heterodimerization, additional co-IP analysis was carried out to confirm the in vivo interactions between BIR1 and BAK1. First, a construct expressing BAK1-3×FLAG protein in pCambia1305 under its native promoter was transformed into plants homozygous for *bkk1* and heterozygous for *bak1*. *bak1 bkk1* homozygous plants carrying the transgene were identified in the T2 generation, and they were found to exhibit wild-type morphology, suggesting that the 3×FLAG tags did not affect BAK1 function. Co-IP using anti-FLAG agarose beads was
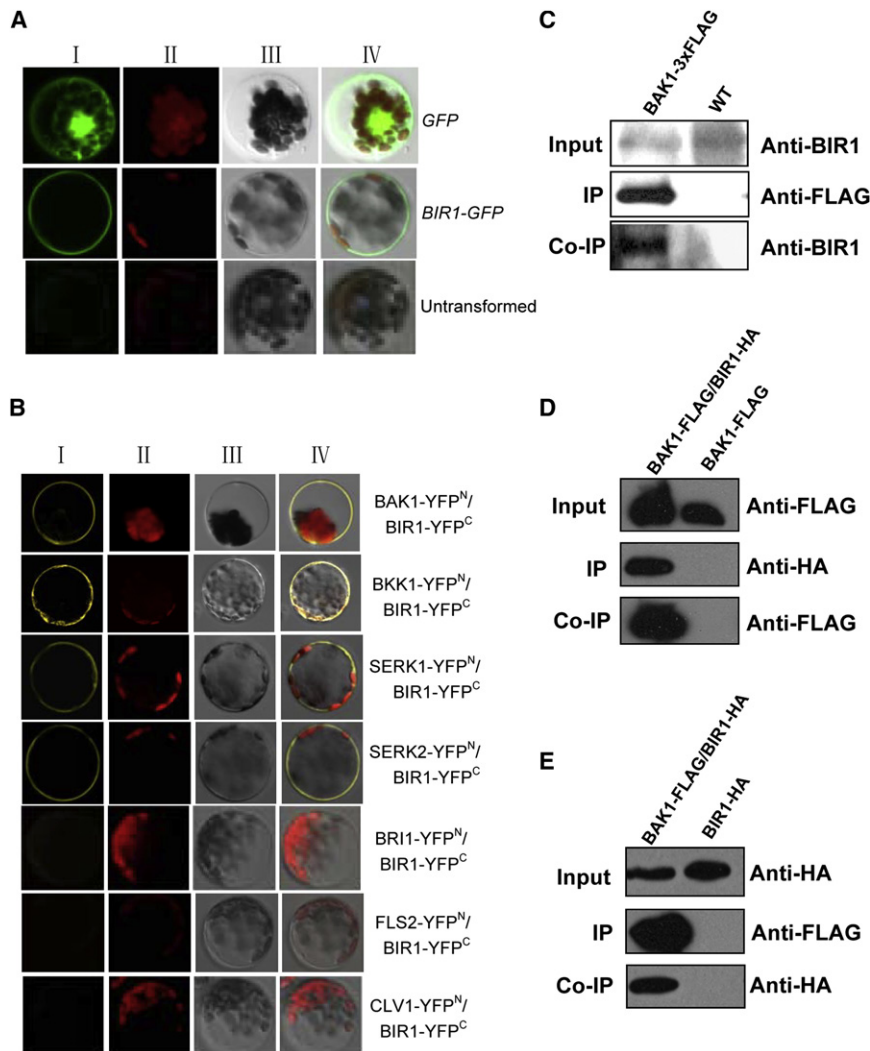
Figure 2. BIR1 Associates with BAK1 In Vivo

(A) Localization of BIR1-GFP fusion protein. *Arabidopsis* mesophyll protoplasts were transfected with a *35S-BIR1-GFP* construct and examined by confocal microscopy 16 hr after transfection. A *35S::GFP* construct and untransformed protoplasts were used as negative control. Epifluorescence (I), chloroplast autofluorescence (II), bright field (III), and merged (IV) are shown.

(B) Analysis of interactions between BIR1 and different RLKs by BiFC analysis. Epifluorescence (I), chloroplast autofluorescence (II), bright field (III), and merged (IV) images of *Arabidopsis* mesophyll protoplasts cotransfected with constructs expressing the BIR1-YFP^C and indicated RLK-YFP^N fusion proteins are shown.

(C) Co-IP of BIR1 with BAK1-3×FLAG in membrane extracts of *BAK1-3×FLAG* transgenic plants. Membrane protein extracts were subjected to immunoprecipitation with anti-FLAG Sepharose beads. Crude lysates (upper panel, Input) and immunoprecipitated proteins (lower panels) were detected with anti-FLAG or anti-BIR1 antibodies.

(D) In vivo pull-down of FLAG-tagged BAK1 by HA-tagged BIR1. *Arabidopsis* mesophyll protoplasts were transfected with *BIR1-3xHA* and *BAK1-3×FLAG* constructs together (lane 1) or the *BAK1-3×FLAG* construct alone (lane 2). Total protein extracts were subjected to immunoprecipitation with anti-HA Sepharose beads. Crude lysates (Input) and immunoprecipitated proteins (lower panels) were detected with anti-HA or anti-FLAG antibodies.

(E) In vivo pull-down of HA-tagged BIR1 by FLAG-tagged BAK1. *Arabidopsis* mesophyll protoplasts were transfected with *BAK1-3×FLAG* and *BIR1-3×HA* constructs together (lane 1) or the *BIR1-3xHA* construct alone (lane 2). Total protein extracts were subjected to immunoprecipitation with anti-FLAG Sepharose beads. Crude lysates (Input) and immunoprecipitated proteins (lower panels) were detected with anti-FLAG or anti-HA antibodies.

subsequently performed on total membrane proteins of these transgenic plants expressing the BAK1-3×FLAG fusion protein. As shown in Figure 2C, BIR1 coimmunoprecipitated with 3×FLAG-tagged BAK1, indicating that BIR1 and BAK1 interact in vivo. As a negative control, immunoprecipitated proteins were also probed with an anti-FLS2 antibody, and no FLS2 was detected in the immunoprecipitated proteins (data not shown).

We also performed co-IP analysis using *Arabidopsis* protoplasts cotransformed with epitope-tagged BIR1 and BAK1. As BIR1 proteins with C-terminal 3×FLAG tags or GFP tag can complement the *bir1-1* mutant phenotypes (Figure S7), the tags were fused to the C terminus of BIR1. When total protein from *Arabidopsis* protoplasts cotransfected with constructs expressing HA-tagged BIR1 and FLAG-tagged BAK1 proteins was incubated with anti-HA Sepharose beads to selectively immunoprecipitate the HA-tagged BIR1, BAK1 coimmunoprecipitated with HA-tagged BIR1, while BAK1 was not immunoprecipitated by itself (Figure 2D). The total protein from protoplasts cotransfected with the constructs expressing HA-tagged BIR1 and

FLAG-tagged BAK1 protein was also incubated with anti-FLAG beads to immunoprecipitate the FLAG-tagged BAK1. As shown in Figure 2E, BIR1 coimmunoprecipitated with FLAG-tagged BAK1 while BIR1 was not immunoprecipitated by itself, further confirming that BIR1 and BAK1 interact in vivo.

Activation of Cell Death and Defense Responses in *bir1-1* Is Partially Dependent on *PAD4* and *EDS1*

To test whether R protein-mediated resistance responses are activated in the *bir1-1* mutant, *bir1-1* was crossed to mutants carrying mutations in positive regulators of R protein-mediated defense, including *ndr1-1*, *eds1-1*, and *pad4-1*. As shown in Figure 3A, *bir1-1 pad4-1* and *bir1-1 eds1-1* double mutant plants are much bigger than the *bir1-1* single mutant plants, indicating that *bir1-1* activates the EDS1 and PAD4-dependent resistance pathway. Interestingly, the *bir1-1 ndr1-1* double mutant is also bigger than the *bir1-1* single mutant (Figure 3A), indicating that the NDR1-dependent resistance pathway may also be activated in the *bir1-1* mutant. The effect of *eds1-1*, *pad4-1*, and *ndr1-1* on the size of *bir1-1* was confirmed by determining the plant
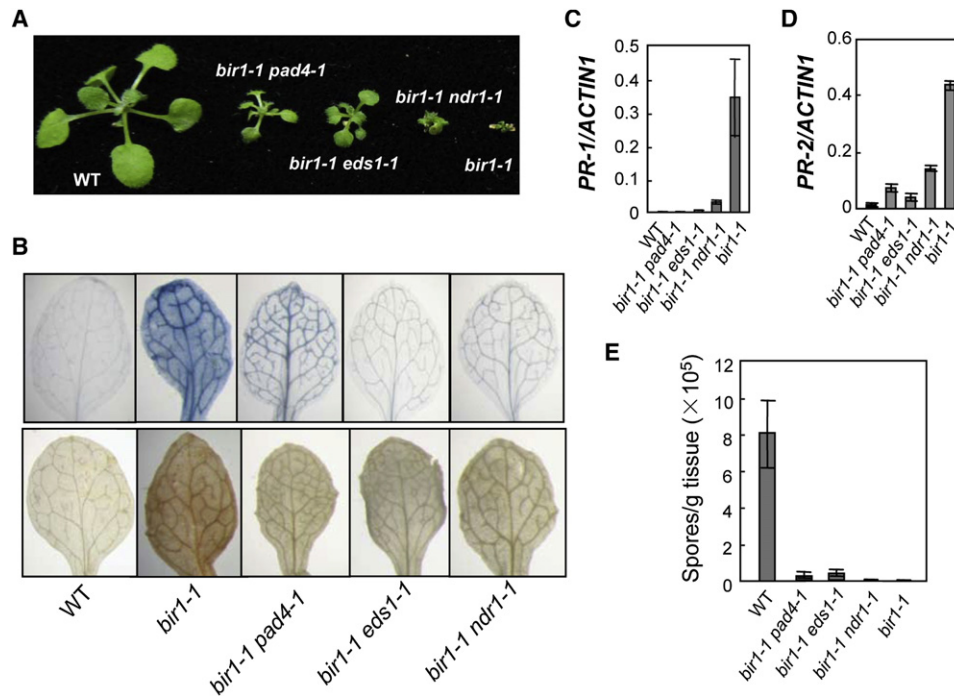
Figure 3. Analysis of *bir1-1 pad4-1*, *bir1-1 eds1-1*, and *bir1-1 ndr1-1* Double Mutants
(A) Morphological phenotypes of wild-type, *bir1-1 pad4-1*, *bir1-1 eds1-1*, *bir1-1 ndr1-1*, and *bir1-1* mutant seedlings. All plants were grown on soil at 22°C in parallel and photographed when they were 3 weeks old.
(B) Trypan blue staining (upper panel) and DAB staining (lower panel) of true leaves of wild-type, *bir1-1 pad4-1*, *bir1-1 eds1-1*, *bir1-1 ndr1-1*, and *bir1-1* mutant.
(C and D) *PR-1* (C) and *PR-2* (D) expression in wild-type, *bir1-1 pad4-1*, *bir1-1 eds1-1*, *bir1-1 ndr1-1*, and *bir1-1* mutant seedlings. Error bars represent SD from averages of three measurements. Values were normalized to the expression of *ACTIN1*.
(E) Growth of *H. p.* Noco2 on wild-type, *bir1-1*, and the respective double mutant plants. Two-week-old seedlings were sprayed with *H. p.* Noco2 spores (10^5 spores/ml). Infection was scored 7 days after inoculation by counting the number of spores per gram of leaf samples. Error bars represent SD from averages of three measurements.

biomass of *bir1-1* single mutant and the double mutants (Figure S10A). Although these double mutants are bigger than *bir1-1*, they still cannot grow to maturity and set seeds at 22°C.

To determine whether cell death in *bir1-1* is dependent on NDR1, EDS1, and PAD4, trypan blue staining was performed on the double mutants. As shown in Figure 3B (upper panel), the double mutants have significantly less cell death compared to the *bir1-1* single mutant. In addition, accumulation of H_2O_2 is reduced in the double mutants (Figure 3B, lower panel). Constitutive expression of *PR-1* and *PR-2* in *bir1-1* was also reduced by mutations in *PAD4*, *EDS1*, and *NDR1* to different degrees (Figures 3C and 3D). Analysis of resistance to *H. p.* Noco2 in the double mutants indicates that constitutive resistance to *H. p.* Noco2 in *bir1-1* was partially compromised by mutations in *PAD4* and *EDS1* but not by the mutation in *NDR1* (Figure 3E). We conclude that knocking out *BIR1* results in activation of multiple resistance pathways that are also activated during R protein-mediated resistance.

Cell Death and Constitutive *PR* Gene Expression in *bir1-1* Are Partially Due to Increased Endogenous SA Levels
SA is an important signal molecule downstream of R protein-mediated resistance responses and mutations in *EDS5*, and *SID2* blocks pathogen-induced SA biosynthesis (Nawrath and Métraux, 1999; Wildermuth et al., 2001). NPR1 is an essential

positive regulator downstream of SA (Durrant and Dong, 2004). To test whether the *bir1-1* mutant phenotypes are dependent on the SA pathway, *bir1-1* was crossed with *eds5-3*, *sid2-1*, and *npr1-3*. Both *eds5-3* and *sid2-1* can partially rescue the *bir1-1* mutant phenotypes (Figure S11A), suggesting that high levels of SA are partly responsible for the *bir1-1* mutant phenotype. The effect of *eds5-3*, *sid2-1*, and *npr1-3* on the size of *bir1-1* was confirmed by determining the plant biomass of *bir1-1* and the double mutants (Figure S10B). In addition, cell death in *bir1-1* is partially blocked by the *eds5-3*, *sid2-1*, and *npr1-3* mutations (Figure S11B). Accumulation of H_2O_2 is also reduced in the double mutants (Figure S11B). Analysis of *PR* gene expression in the double mutant plants showed that constitutive expression of *PR-1* in *bir1-1* was dramatically reduced by mutations in *SID2*, *EDS5*, and *NPR1* (Figures S11C and S11E), but the expression of *PR-2* was not affected by these mutations (Figures S11D and S11F). When the double mutant plants were tested for resistance to *H. p.* Noco2, no significant difference was observed between *bir1-1* and the double mutants (Figure S11G).

Activation of MPK4 by flg22 Is Compromised in *bir1-1*
Like the *bir1-1* mutant, knockout mutants of *Arabidopsis MEKK1* that encode a MAP kinase kinase kinase have temperature-dependent cell death and constitutive activation of defense responses (Ichimura et al., 2006; Nakagami et al., 2006;
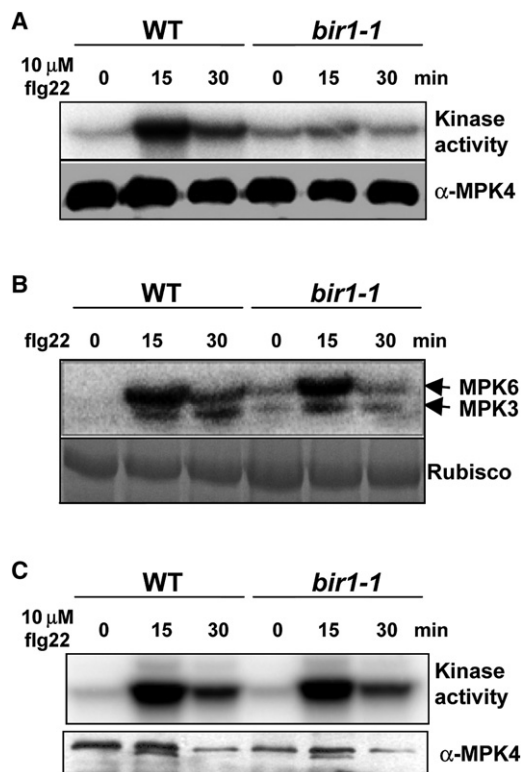
Figure 4. Activities of MAPKs in Wild-Type and the *bir1-1* Mutant

(A) Analysis of MPK4 activity in plants grown at 22°C by immunocomplex kinase assay. Top panel: MPK4 kinase activity. Bottom panel: MPK4 protein levels detected by immunoblot analysis.

(B) Analysis of MPK3 and MPK6 activity in plants grown at 22°C by in-gel kinase assay.

(C) Analysis of MPK4 activity in plants grown at 27°C by immunocomplex kinase assay. Top panel: MPK4 activity. Bottom panel: MPK4 protein levels detected by immunoblot analysis. In both (A) and (B), 2-week-old seedlings grown on 1/2 MS medium at 22°C were used. Plants used in (C) were cultured at 22°C for 6 days and then transferred to 27°C for anther 8 days. Seedlings were treated with 10 μM flg22 for 15 or 30 min and subsequently collected in liquid nitrogen for kinase assays.

Suarez-Rodriguez et al., 2007). The *mpk4* single mutants and *mkk1 mkk2* double mutants were also shown to exhibit temperature-dependent cell death and constitutive activation of defense responses (Gao et al., 2008; Petersen et al., 2000; Qiu et al., 2008). It was suggested that MEKK1, MKK1/MKK2, and MPK4 form a MAP kinase cascade to negatively regulate R protein-mediated resistance pathways. To test whether BIR1 is required for the activation of MPK4 in response to flg22, we analyzed the kinase activity of MPK4 from wild-type and *bir1-1* plants grown at 22°C. Myelin-basic protein was used as substrate for the assay. As shown in Figure 4A, treatment with flg22 resulted in quick activation of MPK4 in wild-type plants but not in the *bir1-1* mutant, suggesting that activation of MPK4 by flg22 is inhibited in the *bir1-1* mutant. In contrast, both MPK3 and MPK6 are still activated in the *bir1-1* mutant (Figure 4B). We further tested the activation of MPK4 in plants grown at 27°C. Interestingly, activation of MPK4 by flg22 is restored in *bir1-1* plants at 27°C (Figure 4C), suggesting that inhibition of MPK4 activation in *bir1-1* is temperature dependent.

Identification of a Suppressor of *bir1-1*

To identify additional components required for cell-death and resistance pathways activated in *bir1-1*, we performed a genetic screen to find mutations that suppress the seedling lethality phenotype of *bir1-1*. Mutants that can grow to maturity and set seeds at 22°C were identified in the M2 population of ethyl methanesulphonate (EMS)-mutagenized *bir1-1 pad4-1* double mutant. A total of 30 mutants were identified as *sobir* (*suppressor of bir1-1*) mutants. *sobir1-1* is one of the most complete suppressors and was analyzed in detail. *sobir1-1 bir1-1 pad4-1* mutant plants displayed wild-type morphology (Figure 5A). Enhanced resistance to *H. p.* Noco2 in *bir1-1 pad4-1* was also blocked by the *sobir1-1* mutation (Figure S12).

SOBIR1 Encodes an RLK

To map the *sobir1-1* mutation, *sobir1-1 bir1-1 pad4-1* (in the Columbia ecotype background) was crossed with Landsberg plants to generate a segregating F2 population. Crude mapping showed that the *sobir1-1* mutation is in a region between marker T16B12 and F4P9 on chromosome 2. Further fine mapping narrowed the *sobir1-1* mutation to a region of about 130 kb between markers F20M17 and F22D22 (Figure 5B). To identify the molecular lesion in *sobir1-1*, a set of PCR fragments covering the region were amplified from *sobir1-1 bir1-1 pad4-1* and sequenced. Comparing the sequences from the mutant with the *Arabidopsis* genome sequence revealed a single C to T mutation in *At2g31880*. This mutation introduces an early stop codon in the protein. Blast analysis shows that *At2g31880* encodes an RLK with four extracellular LRRs and a cytoplasmic kinase domain, suggesting that it could be involved in signal perception and transduction (Figure 5C). A phylogenetic tree including FLS2, BAK1, BIR1, and this protein is shown in Figure S1. The 3′ UTR of *At2g31880* (also named SRRLK [small RNA-generating RLK]) was previously shown to be involved in the generation of natural antisense transcript-associated siRNAs (Katiyar-Agarwal et al., 2007).

To determine whether the other *sobir* mutants also contain mutations in *At2g31880*, DNA of *At2g31880* was amplified from the other 29 mutants by PCR and sequenced. Ten additional *sobir1* mutants were found to contain mutations in *At2g31880* (Figures 5D and S13). Five of these mutants (from *sobir1-1* to *sobir1-5* in the *bir1-1 pad4-1* mutant background) were crossed with *sobir1-1 bir1-1 pad4-1* to test whether they are allelic to *sobir1-1*. No cell death was observed in the F1 plants, and all F1 plants grew to maturity and set seeds. These data suggest that *SOBIR1* is *At2g31880*.

SOBIR1 Suppresses Cell Death and Defense Responses in *bir1-1*

To determine whether *sobir1-1* can suppress the *bir1-1* mutant phenotypes without the presence of *pad4-1*, the *sobir1-1 bir1-1 pad4-1* triple mutant was crossed with wild-type Columbia, and the *sobir1-1 bir1-1* double mutant was identified from the F2 progeny. Unlike *bir1-1* mutant plants, the *sobir1-1 bir1-1* double mutant can grow to maturity and set seeds at 22°C. As shown in Figure 6A, the *sobir1-1 bir1-1* double mutant is much bigger than the *bir1-1* single mutant, but smaller than the wild-type plants, suggesting that *sobir1-1* and *pad4-1* have additive effects on suppression of the *bir1-1* morphology. To determine whether
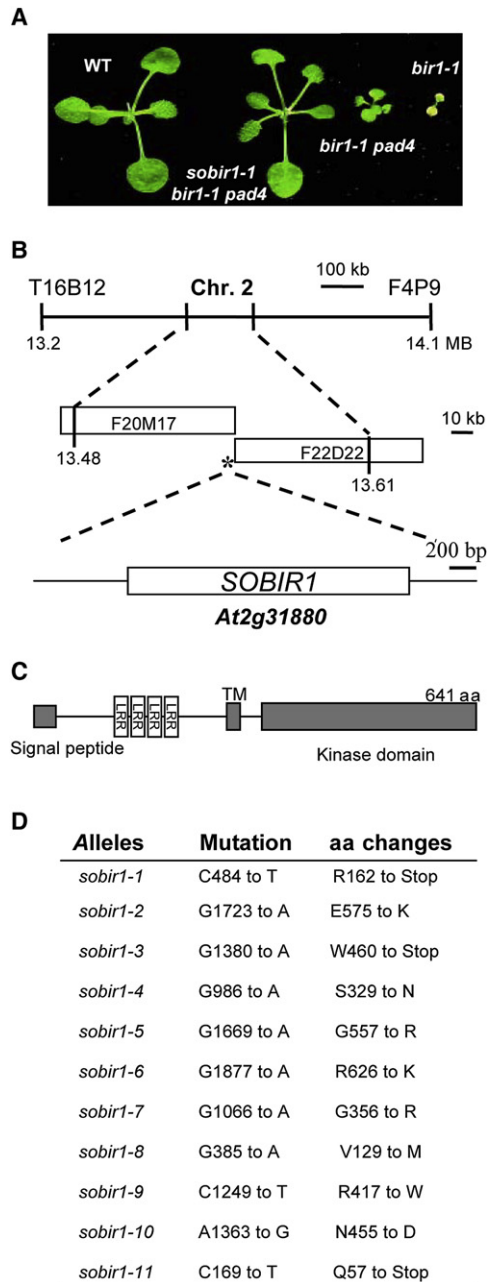
Figure 5. Map-Based Cloning of *sobir1-1*

(A) Morphological phenotypes of wild-type, *sobir1-1 bir1-1 pad4-1*, *bir1-1 pad4-1*, and *bir1-1* plants. Plants were grown on soil at 22°C and photographed 3 weeks after planting.

(B) Map of the *SOBIR1* locus. One recombinant located *sobir1-1* to the south of marker F20M17, and another recombinant located *sobir1-1* to the north of marker F22D22.

(C) Predicted protein structure of the SOBIR1. LRR, leucine-rich repeats; TM, transmembrane motif.
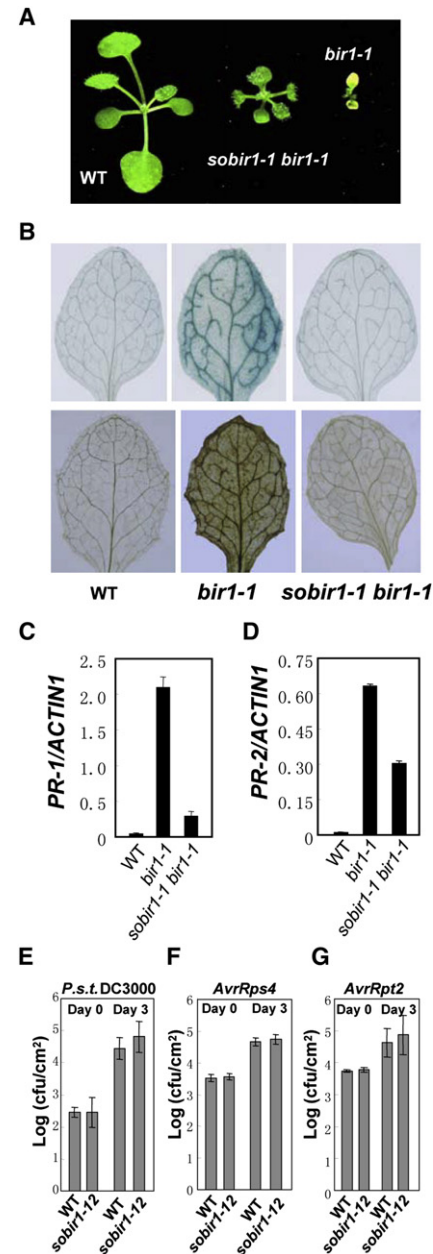
(D) Mutations identified in the *sobir1* alleles.

Figure 6. Characterization of the *sobir1-1 bir1-1* Double Mutant

(A) Phenotypes of wild-type, *sobir1-1 bir1-1*, and *bir1-1* plants. Plants were grown on soil at 22°C and photographed 3 weeks after planting.

(B) Trypan blue staining (top panel) and DAB staining (lower panel) of wild-type, *bir1-1*, and *sobir1-1 bir1-1* mutant seedlings. Whole seedlings were stained with trypan blue or DAB as described (Parker et al., 1996; Thordal-Christensen et al., 1997). Plants were grown at 22°C for 2 weeks on 1/2 MS plates.

(C and D) *PR-1* (C) and *PR-2* (D) expression in the wild-type, *bir1-1*, and *sobir1-1 bir1-1* mutant seedlings. Values were normalized to the expression of *ACTIN1*. Error bars represent SD from averages of three measurements.

(E–G) Growth of *P.s.t.* DC3000 (E), *P.s.t.* DC3000 *AvrRps4* (F), and *AvrRpt2* (G) on wild-type and *sobir1-12* (SALK_050715). Leaves of 5-week-old plants grown at 22°C under 12 hr light/12 hr dark cycles were infiltrated with bacterial suspensions of *P.s.t.* DC3000 (OD_{600} = 0.0002) and *P.s.t.* DC3000 with *AvrRps4* or *AvrRpt2* (OD_{600} = 0.002). The values presented are averages of four replicates ± SD.

cell death was blocked in the *sobir1-1 bir1-1* double mutant, trypan blue staining was performed on the mutant seedlings. As shown in Figure 6B, cell death in *bir1-1* was blocked by the *sobir1-1* mutation. In addition, H_2O_2 accumulation in *bir1-1* is
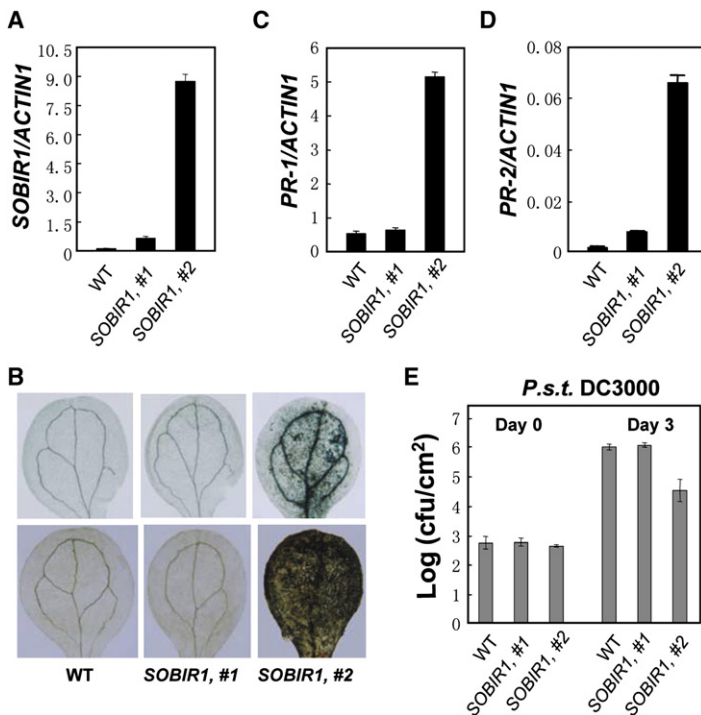
Figure 7. Analysis of Transgenic Plants Overexpressing *SOBIR1*

(A) *SOBIR1* expression in the wild-type and *35S-SOBIR1* transgenic line #1 and line #2. Values were normalized to the expression of *ACTIN1*. Error bars represent SD from averages of three measurements.

(B) Trypan blue staining (top panel) and DAB staining (lower panel) of wild-type and *SOBIR1* transgenic plants. Cotyledons were stained with trypan blue or DAB as described (Parker et al., 1996; Thordal-Christensen et al., 1997).

(C and D) *PR-1* (C) and *PR-2* (D) expression in wild-type and *SOBIR1* transgenic plants. Values were normalized to the expression of *ACTIN1*. Error bars represent SD from averages of three measurements. For analysis performed in (A)–(D), plants were grown at 22°C for 2 weeks on 1/2 MS plates.

(E) Growth of *P.s.t.* DC3000 on wild-type and *SOBIR1* overexpression lines. Leaves of 5-week-old plants were infiltrated with a bacterial suspension at $OD_{600} = 0.0002$. The values presented are averages of four replicates ± SD.

partially affected by the *sobir1-1* mutation (Figure 6B). Expression of both *PR-1* and *PR-2* in *bir1-1* is also significantly reduced by the *sobir1-1* mutation (Figures 6C and 6D).

To test whether *SOBIR1* is required for basal resistance, a knockout mutant of *SOBIR1* (*sobir1-12*) was challenged with *Pseudomonas syringae pv. tomato* (*P.s.t.*) DC3000. As shown in Figure 6E, *sobir1-12* did not exhibit enhanced susceptibility to *P.s.t.* DC3000. Similarly, resistance to *P.s.t.* DC3000 carrying *AvrRPS4* or *AvrRPT2* was not affected in the mutant either (Figures 6F and 6G), suggesting that *SOBIR1* functions as a specific regulator of resistance activated by the *bir1* mutation.

As BIR1 interacts with BAK1 and SOBIR1 encodes an RLK with similar structure as BAK1, we tested whether responses to flg22 are affected in the *sobir1* single mutants. As shown in Figure S14, the *sobir1* mutant plants displayed similar responses to flg22 as wild-type plants, suggesting that SOBIR1 is not required for flg22-mediated resistance responses. We also tested whether SOBIR1 interacts with BIR1 using BiFC analysis. No interaction was found between SOBIR1 and BIR1 (Figure S15). In addition, SOBIR1 and BIR1 did not interact with each other in yeast two-hybrid analysis (data not shown).

Overexpression of *SOBIR1* Activates Cell Death and Defense Responses

Since loss of *SOBIR1* function suppresses cell death in *bir1-1*, *SOBIR1* could be a positive regulator of cell death and innate immunity. To determine whether overexpression of *SOBIR1* activates defense responses, transgenic plants expressing *SOBIR1* under cauliflower mosaic virus 35S promoter were generated. Two representative lines, one with relatively low level of *SOBIR1* expression and one with high level of *SOBIR1* expression, were analyzed in detail. As shown in Figure 7A, *SOBIR1* expression is about 5-fold higher in line #1 and 70-fold higher in line #2

compared to the wild-type. The cotyledons of line #2 but not line #1 die after germination. Trypan blue staining showed that cell death occurred in the cotyledon of line #2, but not in line #1 and the wild-type plants (Figure 7B), suggesting that overexpression of *SOBIR1* leads to activation of cell death. At 22°C, plants from line #2 overexpressing SOBIR1 die when they are about 5–6 weeks old. The cell death in line #2 can be partially suppressed by high temperatures, and plants grown at 28°C can set seeds. As shown in Figures 7C and 7D, both *PR-1* and *PR-2* are constitutively upregulated in line #2 compared to the wild-type plants. Line #2 also displayed enhanced resistance to *P.s.t.* DC3000 (Figure 7E), suggesting that overexpression of *SOBIR1* leads to constitutive activation of pathogen-resistance responses.

DISCUSSION

Activation of R proteins after recognition of effector signals from pathogens often leads to localized cell death. Because constitutive activation of R proteins is detrimental to plants, R protein-mediated signaling pathways must be under tight control. However, it is unclear how the negative regulation is executed. The cell-death phenotype and constitutive activation of defense responses in the *bir1-1* mutant resemble what occurs with constitutive R protein activation. The cell-death phenotype in *bir1-1* is partially dependent on PAD4 and EDS1, proteins required for the functions of many TIR-NB-LRR type of R proteins, suggesting that knocking out *BIR1* activates resistance pathways that are also activated during R protein-mediated resistance. BIR1 may be involved in preventing activation of R protein-mediated resistance when there is no effector activity present. Higher temperatures can often suppress cell death caused by R protein activation (Whitham et al., 1994; Yang and Hua, 2004). Consistent with this hypothesis, cell death in *bir1-1* can also be partially suppressed by higher temperatures.

We found that BAK1 associates with BIR1 in vivo, suggesting that BAK1 works together with BIR1 to negatively regulate cell death and defense responses. In *Arabidopsis*, BAK1 is involved in the perception of multiple signals. BAK1 participates in the

perception of BRs through association with BRI1 (Li et al., 2002; Nam and Li, 2002). At the same time, BAK1 associates with FLS2 and is required for the perception of bacterial flagellin and PAMP-mediated activation of innate immune responses (Chinchilla et al., 2007; Heese et al., 2007). Unlike FLS2 and BRI1, which contain long extracellular LRR repeats, BIR1 has only five LRRs. It is unclear whether the BIR1 and BAK1 complex functions in signal perception. If it is involved in the perception of an unknown signal, the signal is most likely endogenous, since cell death occurs in *bir1-1* and *bak1 bkk1-1* mutants even under sterile conditions.

On one hand, BAK1 functions as a positive regulator of PAMP-induced immunity. On the other hand, BAK1 serves as a negative regulator of R protein-mediated immunity. Our data suggest that BAK1 may be a general coreceptor for multiple RLKs that function in different biological processes. The specificity of BAK1 in these processes is determined by the RLKs BAK1 interacts with. The positive role of BAK1 in flagellin-induced immunity is accomplished by its association with FLS2, while the negative regulation of R protein-mediated resistance is carried out by its association with BIR1. One possibility is that the BAK1 and BIR1 complex is the guardee of one or more R proteins. Loss of the BAK1 or BIR1 function triggers the activation of these R proteins.

To elucidate the resistance pathways activated in the *bir1-1* mutant, a suppressor screen of *bir1-1* was performed. One of the mutants, *sobir1-1*, was found to suppress the seedling lethality phenotype of *bir1-1*. While *sobir1-1* suppresses cell death in *bir1-1*, overexpression of *SOBIR1* leads to activation of cell death, indicating that *SOBIR1* is a critical positive regulator of cell death. Combining the *sobir1-1* and *pad4-1* mutations results in complete suppression of cell death, H_2O_2 accumulation, *PR* gene expression, and pathogen resistance in *bir1-1*, suggesting that *SOBIR1* functions in parallel with *PAD4* to regulate cell death and defense responses. Interestingly, *SOBIR1* encodes another RLK, suggesting that there is a *SOBIR1*-dependent signal transduction pathway activated in *bir1-1* to promote cell death and disease resistance.

To explain the BIR1-mediated negative regulation of resistance responses, a simple working model is proposed in Figure S16. When plants are not attacked by pathogens, BIR1 or the BIR1 and BAK1/SERKs protein complex is guarded by two or multiple hypothetical R proteins. Loss of the function of BIR1 leads to activation of these R proteins. The first R protein is in the TIR-NB-LRR class that activates the *PAD4*-dependent resistance pathway. The second R protein probably belongs to a different class that activates the *SOBIR1*-dependent resistance pathway. Blocking the *PAD4* and *SOBIR1*-dependent resistance pathways together reverts the *bir1-1* mutant back to wild-type. Future characterization of the other *sobir* mutants and cloning of the mutant genes will help us better understand how the *SOBIR1*-dependent resistance pathway is regulated.

EXPERIMENTAL PROCEDURES

Plant Materials and Growth Conditions
Plants were grown at 22°C under 16 hr light/8 hr dark. Seeds of *bir1-1* (WiscDsLox393-396D17) were obtained from the *Arabidopsis* Stock Center (ABRC; Ohio State University; Columbus, OH). The homozygous plants were

obtained by PCR using primers BIR1-179F and BIR1-891R. To generate various double mutants, the *bir1-1/BIR1* heterozygous plants were crossed with homozygous *pad4-1*, *eds1-1*, *ndr1-1*, *sid2-1*, *eds5-3*, and *npr1-3*. The F1 plants heterozygous for *bir1-1* T-DNA were identified by PCR. Double mutant plants were identified in the F2 progeny by PCR.

Plasmid Construction and *Arabidopsis* Transformation
For complementation analysis, a 4.6 kb genomic DNA fragment containing *BIR1* was amplified by PCR using primers BIR1-GF and BIR1-GR and cloned into binary vector pCAMBIA1300 to create pCAMBIA1300-BIR1g. A similar genomic DNA fragment lacking the stop codon and 3′-UTR region was amplified by PCR using primers BIR1-GF and BIR1-FLAG-R and cloned into a modified pCAMBIA1305 vector with a 3×FLAG tag to obtain pCAMBIA1305-BIR1-3×FLAG for expressing the BIR1 3×FLAG-tag fusion protein under its native promoter. To confirm that the phenotypes observed in *bir1-1* were caused by mutation in *BIR1*, pCAMBIA1300-BIR1g and pCAMBIA1305-BIR1-3×FLAG were transformed into *Agrobacterium* and subsequently into the *BIR1/bir1-1* heterozygous plants by floral dipping (Clough and Bent, 1998). Homozygous *bir1-1* plants carrying the transgene were identified in the T2 generation with Hygromycin selection and PCR.

For BiFC study, the *BIR1*, *BAK1*, *BKK1*, *SERK1*, *SERK2*, *BRI1*, and *CLV1* cDNA were amplified by RT-PCR from wild-type Columbia. *BIR1* was cloned into pUC-SPYCE to obtain pBIR1-YCE using primers BIR1-YCE-F and BIR1-FLAG-R. *BAK1*, *BKK1*, *SERK1*, and *SERK2* were cloned into pUC-SPYNE to obtain pBAK1-YNE, pBKK1-YNE, pSERK1-YNE, and pSERK2-YNE using primers BAK1-YNE-F, BAK1-YNE-R, BKK1-YNE-F, BKK1-YNE-R, SERK1-YNE-F, SERK1-YNE-R, SERK2-YNE-F, and SERK2-YNE-R. *BRI1* and *CLV1* were also cloned into pUC-SPYNE to obtain pBRI1-YNE and pCLV1-YNE using primers BRI1-F, BRI1-R, CLV1-F, and CLV1-R. pFLS2-YNE was kindly provided by Dr. Zhou Jianmin.

The *BIR1* and *BAK1* cDNA were also amplified for making constructs for co-IP analysis. *BIR1* was cloned into pUC-3xHA with 35S promoter to create pBIR1-3HA using primers BIR1-A and BIR1-FLAG-R. *BAK1* was cloned to pUC-3×FLAG with 35S promoter to obtain pBAK1-3×FLAG using primers BAK1-A and BAK1-B. For localization analysis, *BIR1* cDNA was amplified by PCR using primers BIR1-GFP-A and BIR1-FLAG-R and cloned into pCAMBIA1300-35S-GFP to obtain p35S-BIR1-GFP. For overexpression of *SOBIR1*, the *SOBIR1* cDNA was amplified by PCR and cloned into a modified pCAMBIA1300 vector with 35S promoter to obtain p35S-SOBIR1. Sequences of primers used are listed in Table S2. All constructs were confirmed by sequencing.

Localization and BiFC Analysis
For transient expression of the YFP[N] and YFP[C] fusion proteins, constructs expressing BIR1-YFP[C], BAK1-YFP[N], and various control proteins were cotransfected into *Arabidopsis* mesophyll protoplasts according to a previously described protocol (Sheen, 2001). YFP fluorescence was observed by confocal microscopy.

Co-IP Analysis
For co-IP analysis of interactions between BIR1 and BAK1, *Arabidopsis* mesophyll protoplasts or membrane fractions of plant seedlings were extracted in extraction buffer (50 mM HEPES-KOH [pH 7.4], 150 mM NaCl, 5 mM NaF, 1 mM Na_3VO_4, 0.5% Triton X-100, 0.5 mM DTT, 1 mM PMSF, 1× PI cocktail). After centrifugation at 13,000 rpm for 15 min, anti-HA antibody (Roche) or anti-FLAG antibody (Sigma) was added to the supernatant and incubated for 1 hr at 4°C. Twenty microliters of protein A Sepharose beads (Sigma) were subsequently added and incubated for another 3 hr at 4°C. After washing the beads eight times with extraction buffer, immunoprecipitates were analyzed by western blot analyses. The polyclonal anti-BIR1 antibody was generated in rabbit using a fragment of the BIR1 kinase domain-expressed *E. coli*. The antibody detects a protein about 80 kDa specifically present in wild-type plants.

Mutant Screen and Characterization
Seeds of *bir1-1 pad4-1* were obtained by growing the plants at 28°C and mutagenized with EMS. About 12,000 M2 plants were screened to identify mutants that can grow to maturity and set seeds at 22°C. The *sobir1-1 bir1-1 pad4-1* mutant was backcrossed with wild-type Columbia. The

sobir1-1 single mutant and the *sobir1-1 bir1-1* double mutant were identified among the F2 progeny by PCR genotyping.

Expression of *PR* genes was analyzed as previously described (Zhang et al., 2003b). Trypan blue and DAB staining were performed on 2-week-old seedlings grown on 1/2 MS medium according to previously described procedures (Parker et al., 1996; Thordal-Christensen et al., 1997).

SUPPLEMENTAL DATA

Supplemental Data include Supplemental Experimental Procedures, Supplemental References, 16 Figures, and two tables and can be found online at http://www.cell.com/cell-host-microbe/supplemental/S1931-3128(09)00190-5.

REFERENCES

Aarts, N., Metz, M., Holub, E., Staskawicz, B.J., Daniels, M.J., and Parker, J.E. (1998). Different requirements for EDS1 and NDR1 by disease resistance genes define at least two R gene-mediated signaling pathways in Arabidopsis. Proc. Natl. Acad. Sci. USA *95*, 10306–10311.

Bendahmane, A., Farnham, G., Moffett, P., and Baulcombe, D.C. (2002). Constitutive gain-of-function mutants in a nucleotide binding site-leucine rich repeat protein encoded at the Rx locus of potato. Plant J. *32*, 195–204.

Century, K.S., Holub, E.B., and Staskawicz, B.J. (1995). NDR1, a locus of Arabidopsis thaliana that is required for disease resistance to both a bacterial and a fungal pathogen. Proc. Natl. Acad. Sci. USA *92*, 6597–6601.

Chinchilla, D., Zipfel, C., Robatzek, S., Kemmerling, B., Nürnberger, T., Jones, J.D., Felix, G., and Boller, T. (2007). A flagellin-induced complex of the receptor FLS2 and BAK1 initiates plant defence. Nature *448*, 497–500.

Clough, S.J., and Bent, A.F. (1998). Floral dip: a simplified method for Agrobacterium-mediated transformation of Arabidopsis thaliana. Plant J. *16*, 735–743.

Dong, M.Q., Venable, J.D., Au, N., Xu, T., Park, S.K., Cociorva, D., Johnson, J.R., Dillin, A., and Yates, J.R., 3rd. (2007). Quantitative mass spectrometry identifies insulin signaling targets in C. elegans. Science *317*, 660–663.

Durrant, W.E., and Dong, X. (2004). Systemic acquired resistance. Annu. Rev. Phytopathol. *42*, 185–209.

Feys, B.J., Wiermer, M., Bhat, R.A., Moisan, L.J., Medina-Escobar, N., Neu, C., Cabral, A., and Parker, J.E. (2005). Arabidopsis SENESCENCE-ASSOCIATED GENE101 stabilizes and signals within an ENHANCED DISEASE SUSCEPTIBILITY1 complex in plant innate immunity. Plant Cell *17*, 2601–2613.

Gao, M., Liu, J., Bi, D., Zhang, Z., Cheng, F., Chen, S., and Zhang, Y. (2008). MEKK1, MKK1/MKK2 and MPK4 function together in a mitogen-activated protein kinase cascade to regulate innate immunity in plants. Cell Res. *18*, 1190–1198.

Glazebrook, J., Rogers, E.E., and Ausubel, F.M. (1996). Isolation of Arabidopsis mutants with enhanced disease susceptibility by direct screening. Genetics *143*, 973–982.

Gomez-Gomez, L., and Boller, T. (2000). FLS2: an LRR receptor-like kinase involved in the perception of the bacterial elicitor flagellin in Arabidopsis. Mol. Cell *5*, 1003–1011.

He, K., Gou, X., Yuan, T., Lin, H., Asami, T., Yoshida, S., Russell, S.D., and Li, J. (2007). BAK1 and BKK1 regulate brassinosteroid-dependent growth and brassinosteroid-independent cell-death pathways. Curr. Biol. *17*, 1109–1115.

Heese, A., Hann, D.R., Gimenez-Ibanez, S., Jones, A.M., He, K., Li, J., Schroeder, J.I., Peck, S.C., and Rathjen, J.P. (2007). The receptor-like kinase SERK3/BAK1 is a central regulator of innate immunity in plants. Proc. Natl. Acad. Sci. USA *104*, 12217–12222.

Horn, M.A., and Walker, J.C. (1994). Biochemical properties of the autophosphorylation of RLK5, a receptor-like protein kinase from Arabidopsis thaliana. Biochim. Biophys. Acta *1208*, 65–74.

Ichimura, K., Casais, C., Peck, S.C., Shinozaki, K., and Shirasu, K. (2006). MEKK1 is required for MPK4 activation and regulates tissue-specific and temperature-dependent cell death in Arabidopsis. J. Biol. Chem. *281*, 36969–36976.

Jones, J.D., and Dangl, J.L. (2006). The plant immune system. Nature *444*, 323–329.

Katiyar-Agarwal, S., Gao, S., Vivian-Smith, A., and Jin, H. (2007). A novel class of bacteria-induced small RNAs in Arabidopsis. Genes Dev. *21*, 3123–3134.

Kemmerling, B., Schwedt, A., Rodriguez, P., Mazzotta, S., Frank, M., Qamar, S.A., Mengiste, T., Betsuyaku, S., Parker, J.E., Müssig, C., et al. (2007). The BRI1-associated kinase 1, BAK1, has a brassinolide-independent role in plant cell-death control. Curr. Biol. *17*, 1116–1122.

Li, J., Wen, J., Lease, K.A., Doke, J.T., Tax, F.E., and Walker, J.C. (2002). BAK1, an Arabidopsis LRR receptor-like protein kinase, interacts with BRI1 and modulates brassinosteroid signaling. Cell *110*, 213–222.

Li, X., Zhang, Y., Clarke, J.D., Li, Y., and Dong, X. (1999). Identification and cloning of a negative regulator of systemic acquired resistance, SNI1, through a screen for suppressors of npr1-1. Cell *98*, 329–339.

Mackey, D., Belkhadir, Y., Alonso, J.M., Ecker, J.R., and Dangl, J.L. (2003). Arabidopsis RIN4 is a target of the type III virulence effector AvrRpt2 and modulates RPS2-mediated resistance. Cell *112*, 379–389.

Nakagami, H., Soukupová, H., Schikora, A., Zársky, V., and Hirt, H. (2006). A Mitogen-activated protein kinase kinase kinase mediates reactive oxygen species homeostasis in Arabidopsis. J. Biol. Chem. *281*, 38697–38704.

Nam, K.H., and Li, J. (2002). BRI1/BAK1, a receptor kinase pair mediating brassinosteroid signaling. Cell *110*, 203–212.

Nawrath, C., and Métraux, J.-P. (1999). Salicylic acid induction-deficient mutants of Arabidopsis express PR-2 and PR-5 and accumulate high levels of camalexin after pathogen inoculation. Plant Cell *11*, 1393–1404.

Noutoshi, Y., Ito, T., Seki, M., Nakashita, H., Yoshida, S., Marco, Y., Shirasu, K., and Shinozaki, K. (2005). A single amino acid insertion in the WRKY domain of the Arabidopsis TIR-NBS-LRR-WRKY-type disease resistance protein SLH1 (sensitive to low humidity 1) causes activation of defense responses and hypersensitive cell death. Plant J. *43*, 873–888.

Parker, J.E., Holub, E.B., Frost, L.N., Falk, A., Gunn, N.D., and Daniels, M.J. (1996). Characterization of eds1, a mutation in Arabidopsis suppressing resistance to Peronospora parasitica specified by several different RPP genes. Plant Cell *8*, 2033–2046.

Petersen, M., Brodersen, P., Naested, H., Andreasson, E., Lindhart, U., Johansen, B., Nielsen, H.B., Lacy, M., Austin, M.J., Parker, J.E., et al. (2000). Arabidopsis map kinase 4 negatively regulates systemic acquired resistance. Cell *103*, 1111–1120.

Qiu, J.-L., Zhou, L., Yun, B.-W., Nielsen, H.B., Fiil, B.K., Petersen, K., Mackinlay, J., Loake, G.J., Mundy, J., and Morris, P.C. (2008). Arabidopsis mitogen-activated protein kinase kinases MKK1 and MKK2 have overlapping functions in defense signaling mediated by MEKK1, MPK4, and MKS1. Plant Physiol. *148*, 212–222.

Ranish, J.A., Yi, E.C., Leslie, D.M., Purvine, S.O., Goodlett, D.R., Eng, J., and Aebersold, R. (2003). The study of macromolecular complexes by quantitative proteomics. Nat. Genet. *33*, 349–355.

Shan, L., He, P., Li, J., Heese, A., Peck, S.C., Nürnberger, T., Martin, G.B., and Sheen, J. (2008). Bacterial effectors target the common signaling partner BAK1 to disrupt multiple MAMP receptor-signaling complexes and impede plant immunity. Cell Host Microbe *4*, 17–27.

Sheen, J. (2001). Signal transduction in maize and Arabidopsis mesophyll protoplasts. Plant Physiol. *127*, 1466–1475.

Shirano, Y., Kachroo, P., Shah, J., and Klessig, D.F. (2002). A gain-of-function mutation in an Arabidopsis Toll Interleukin1 receptor-nucleotide binding site-leucine-rich repeat type R gene triggers defense responses and results in enhanced disease resistance. Plant Cell *14*, 3149–3162.

Suarez-Rodriguez, M.C., Adams-Phillips, L., Liu, Y., Wang, H., Su, S.H., Jester, P.J., Zhang, S., Bent, A.F., and Krysan, P.J. (2007). MEKK1 is required for flg22-induced MPK4 activation in Arabidopsis plants. Plant Physiol. *143*, 661–669.

Thordal-Christensen, H., Zhang, Z., Wei, Y., and Collinge, D.B. (1997). Subcellular localization of H2O2 in plants. H2O2 accumulation in papillae and hypersensitive response during the barley-powdery mildew interaction. Plant J. *11*, 1187–1194.

Van der Biezen, E.A., and Jones, J.D. (1998). Plant disease-resistance proteins and the gene-for-gene concept. Trends Biochem. Sci. *23*, 454–456.

Walter, M., Chaban, C., Schütze, K., Batistic, O., Weckermann, K., Nake, C., Blazevic, D., Grefen, C., Schumacher, K., Oecking, C., et al. (2004). Visualization of protein interactions in living plant cells using bimolecular fluorescence complementation. Plant J. *40*, 428–438.

Whitham, S., Dinesh-Kumar, S.P., Choi, D., Hehl, R., Corr, C., and Baker, B. (1994). The product of the tobacco mosaic virus resistance gene N: similarity to toll and the interleukin-1 receptor. Cell *78*, 1101–1115.

Wildermuth, M.C., Dewdney, J., Wu, G., and Ausubel, F.M. (2001). Isochorismate synthase is required to synthesize salicylic acid for plant defence. Nature *414*, 562–565.

Yang, S., and Hua, J. (2004). A haplotype-specific Resistance gene regulated by BONZAI1 mediates temperature-dependent growth control in Arabidopsis. Plant Cell *16*, 1060–1071.

Zhang, Y., Goritschnig, S., Dong, X., and Li, X. (2003a). A gain-of-function mutation in a plant disease resistance gene leads to constitutive activation of downstream signal transduction pathways in suppressor of npr1-1, constitutive 1. Plant Cell *15*, 2636–2646.

Zhang, Y., Tessaro, M.J., Lassner, M., and Li, X. (2003b). Knockout analysis of Arabidopsis transcription factors TGA2, TGA5, and TGA6 reveals their redundant and essential roles in systemic acquired resistance. Plant Cell *15*, 2647–2653.

Zipfel, C., Kunze, G., Chinchilla, D., Caniard, A., Jones, J.D., Boller, T., and Felix, G. (2006). Perception of the bacterial PAMP EF-Tu by the receptor EFR restricts Agrobacterium-mediated transformation. Cell *125*, 749–760.